Applied Physics B (2020) 126:127
https://doi.org/10.1007/s00340-020-07481-w

Applied Physics B
Lasers and Optics

3.5 ps burst mode pulses based on all-normal dispersion harmonic mode-locked

Haolin Yang[1] · Yue Chen[1] · Kaili Ding[1] · Fuqiang Jia[1] · Kang Li[2] · Nigel Copner[2]

Received: 22 December 2019 / Accepted: 29 June 2020 / Published online: 8 July 2020

Abstract
A polarization-maintaining (PM) fiber-coupled acousto-optic modulator (AOM) was used, in the present work, to tailor the stable 3.523 picosecond (ps) mode-locked pulses generated by an all PM fiber oscillator. The pulse clusters with 7.315 MHz, 731.5 kHz, and 73.15 kHz of repetition rate were obtained. The number of pulses in each pulse cluster could be adjusted from 1 to 6. Through the harmonic mode-locked (HML) technology, the tunability of the fiber laser was remarkably improved. Ultimately, the tunable number of pulses were extended to 8, 10, and 12, and obtained 4, 6 and 8 pulses with equal amplitude respectively, providing a greater flexibility than previous methods.

1 Introduction

In metal micro-machining applications, ultra-fast burst mode lasers with few picosecond in pulse width, are ideal for precise machining of metals [1–3] Dausinger et al. proved that a pulse duration near 5–10 ps appears to be optimal for micro-machining of metals, since it minimizes the thermal damage and avoids disturbing nonlinear effects [4, 5]. Joribanks et al. first used an ultra-fast burst pulses to remove ablation material in 1999 successfully [6]. By applying burst mode to ultra-fast lasers, both the repetition rate and the number of pulses in each pulse cluster can be modulated [7–9]. Several methods can be applied to generate burst pulses. One of these methods is the use of a Michelson interferometer [10–12], but the configuration is complex. Another method is the use of active devices, such as electro-optic modulator (EOM) and AOM, to tailor the pulse trains from master oscillator (seed source) [13–16]. However, the burst pulses reported in these reports have a common problem, which is unequal pulse amplitudes in each pulse cluster.

All-fiber ultra-fast burst mode lasers own better stability and more straightforward configuration. In Table 1, we list a number of picosecond seed sources which are capable of generating burst mode laser. These seed sources operated in all-normal dispersion (ANDi) regime, the pulses would be affected by the combined effects of the positive group-velocity dispersion (GVD) and the nonlinearity. Therefore, without any pulse compression or dispersion compensation, the pulse width obtained were wider than 10 ps.

In this present work, the all PM fiber picosecond laser, achieved in our work, not only had a <5 ps of pulse width optimized for micro-machining, but also owned a flexible controllability of the burst mode laser. Apart from the burst pulses, we also achieved the ANDi HML based on a SESAM. Although many reports about the ANDi HML had already reported, these reports focused on using nonlinear polarization (NPR) [24–29], nonlinear amplifying mirrors (NAML) [30] and graphene oxide saturable absorber (SA) [31], and the structures used were complex.

2 Experimental setups

The configuration of picosecond burst mode pulse laser, as schematically demonstrated in Fig. 1, consists of two parts: an oscillator and a pre-amplifier. The oscillator used a 0.5 m single mode PM ytterbium doped (Yb-doped) fiber (Nufern PM-YSF-HI-HP, peak core absorption of

✉ Haolin Yang
23120171153004@stu.xmu.edu.cn

Fuqiang Jia
jiafq@xmu.edu.cn

Kang Li
kang.li@southwales.ac.uk

[1] School of Electronic Science and Engineering, Xiamen University, Fujian 361005, Xiamen, China

[2] Wireless and Optoelectronics Research and Innovation Centre, Faculty of Computing, Engineering and Science, University of South Wales, Wales, UK

Table 1 Some representative experimental results of mode-locked picosecond fiber lasers

Years	Cavity length (m)	Repetition rate (MHz)	Pulse width (ps)	Dispersion compensation/pulse compress	References
2004	158 cm	95	1.5	Yes	[17]
2008	3	50	3.8	Yes	[18]
2009	500	191 kHz	2	No	[19]
2011	5	30	15	Yes	[20]
2012	~20 cm	843	21	No	[21]
2012	4.26	35.2	11	No	[22]
2012	19.5	7.7	48.8	No	[22]
2012	4.28	35	26	No	[22]
2012	–	–	0.76	Yes	[22]
2012	3.75	40	457 fs	Yes	[23]
2019	2	73.15	3.523	–	This work

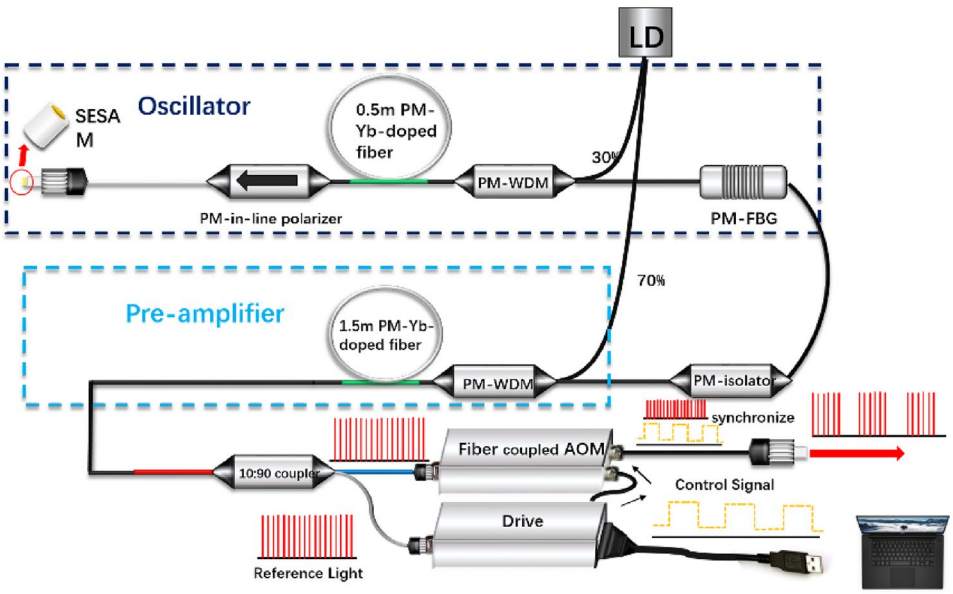

Fig. 1 Configuration of the experimental setups: *PM-WDM* polarization-maintaining wavelength-division-multiplexer coupler, *PM-FBG* polarization-maintaining fiber Bragg grating, *PM-YDF* polarization-maintaining ytterbium doped fiber, *PM-isolator* polarization-maintaining isolator

250 dB/m@975 nm) as a gain medium. A high-reflectivity (90%) fiber Bragg grating (FBG) with 0.71 nm bandwidth was used as an output coupler. A PM in-line polarizer was placed in laser cavity to keep the polarization state. A SESAM (Batop Gmbh SAM-1064-30-8 ps) was placed at the end of the cavity. The pre-amplifier with a 1.5 m PM Yb-doped gain fiber amplified the laser so that it can be responded by an auto-correlator. The 976 nm laser diode (LD) with 350 mW of available power was used to pump the oscillator and the pre-amplifier simultaneously. The length of oscillator was around 2 m corresponding to the ~0.043 ps^2 of total GVD, indicating the fiber laser was running in ANDi regime. The amplified laser was split by a 10:90 fiber coupler and injected into the fiber-coupled AOM and AOM's drive respectively. Signals, detected by the photo detector (PD) integrated in the driver, were used as a reference light. The driver would synchronize the modulator window with the reference light automatically. The signals (delay signal, window width signal, and division frequency signal), sent to the fiber coupled AOM, would modulate the repetition rate of pulse clusters and the number of pulses in each pulse cluster.

3 Results and discussions

Stable mode-locked pulse trains are shown in Fig. 2a. The 13.67 ns of repetition period indicated the laser was running at 73.15 MHz of repetition rate ($f = 1/T$). Figure 2b shows that the signal noise ratio (SNR) in frequency spectrum was about 55 dB. The pulse width was characterized by an auto-correlator. The autocorrelation trace is shown in Fig. 3a.

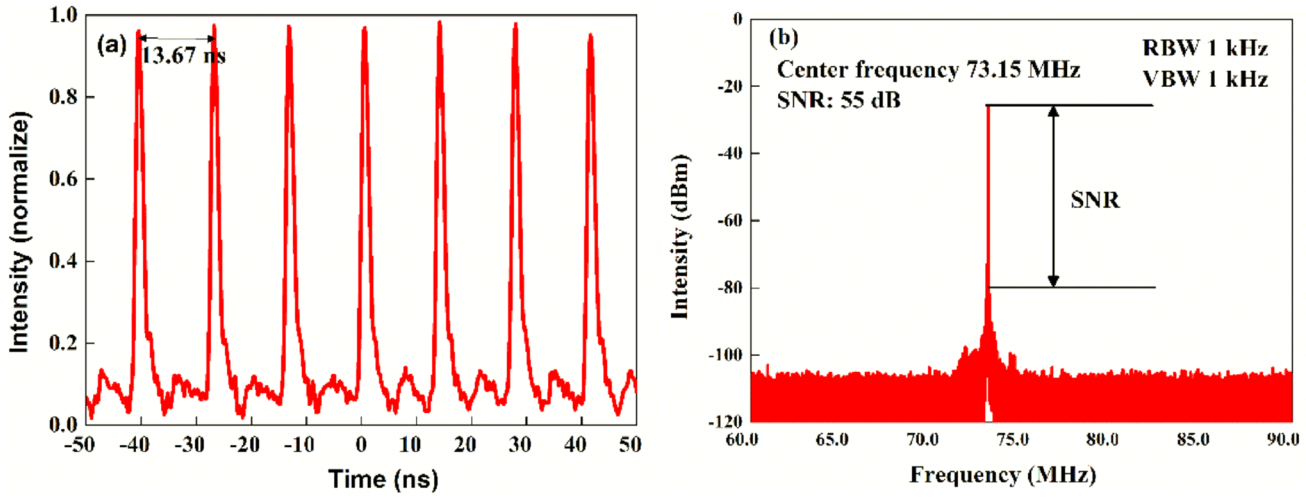

Fig. 2 **a** Mode-locked pulse trains and **b** frequency spectrum of mode- locked pulse trains

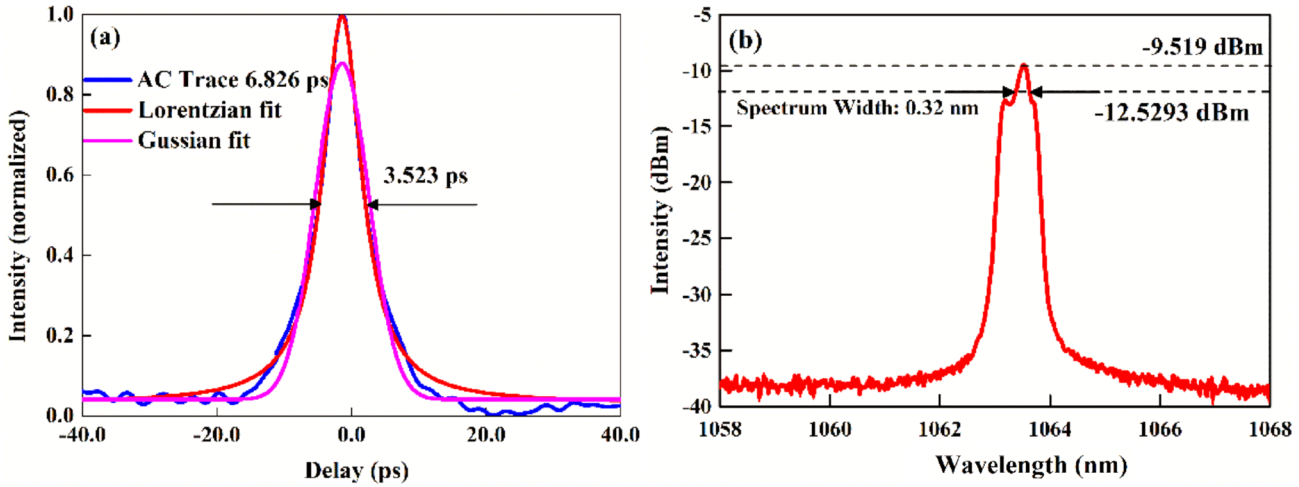

Fig. 3 **a** Autocorrelation trace of the mode-locked laser at 73.15 MHz repetition rate, **b** optical spectrum of the stable mode-locked pulse trains

The auto-correlator fit (ACF) was 6.826 ps. A Lorentzian pulse profile was assumed because Lorentzian fit was better than Gaussian fit as shown as Fig. 3a, the pulse width was ~ 3.523 ps. In Fig. 3b, a 0.32 nm spectrum width was measured by an optical spectral analyzer (ANDO AQ-6315A). According to the value of pulse width and spectrum width, the time-bandwidth-product calculated was about 0.299 which was large than 0.221 of the transform-limited time-bandwidth product for Lorentzian profile, indicating the pulses had some chirp. The noise of ACF can be attributed to the environmental noise. The laser exhibited 19.7 dB of polarization extinction ratio.

Figure 4 illustrates the evolution of the output power. As the pump power increased, the fiber laser operated from a Q-switched mode-locked (QML) state to a continuous wave mode-locked (CWML) state. When the pump power was between 112.4 and 150.4 mW, the laser worked in the QML regime. While, as the pump power exceeded 150.4 mW, the laser was the CWML state and stable for dozens of hours. In ANDi regime, due to the pulse broadening effect resulted from the large positive GVD and nonlinearity, mode-locking process may be unstable and difficult to self-start [32, 33]. In order to balance this effect, the filter with a narrow bandwidth plays an important role [34, 35]. Due to the accumulated nonlinear phase $\Phi_{NL} \propto P_{in}L$ [36], reducing the fiber length favors stable CWML in ANDi regime against multiple pulses breakdown. However, reducing cavity length blindly not only fails to maintain a certain nonlinear phase shift, but also cannot keep the enough intracavity energy

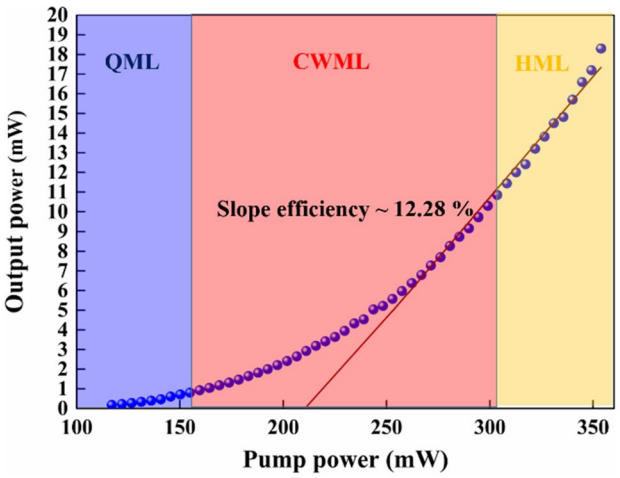

Fig. 4 Output power versus pump power

to reach the threshold for stable CWML against Q-switching instabilities [37]. Utilizing the FBG with a narrow bandwidth to broaden the pulses in time domain is a possible way due to the intracavity peak power $P_{\text{in}} \propto E_{\text{in}}/\tau$. Therefore, the length of the oscillator we designed was 2 m, and we selected the FBG with a narrow bandwidth (0.71 nm) and a high reflectivity (90%) as the output coupler. The threshold for the intracavity pulse energy E_{P}, above which CWML laser is achieved, can be expressed as follow [38]:

$$E_{\text{p,in}}^2 = \frac{F_{\text{sat,A}} A_{\text{A}} \Delta R}{\frac{1}{F_{\text{sat,L}} A_{\text{L}}} + \frac{1}{F_{\text{TPA}} A_{\text{A}}}}, \tag{1}$$

where the saturation fluence of the gain medium is given as $F_{\text{sat,L}} = h\nu/2\sigma$, σ is the emission cross section of the gain medium ($\sim 0.3 \times 10^{-24}$ m^2), A is the laser mode area on the gain medium or SESAM, $F_{\text{sat,A}}$ is the saturation fluence of the SESAM (97 μJ/cm^2), ΔR is the modulation depth of the SESAM (~ 0.13). F_{TPA} is the two-photon absorption of the SESAM (~ 27 mJ/cm^2). According (1), the $E_{\text{p,in}}$ estimated was 0.07 nJ lower than the experimentally measured ~ 0.14 nJ intracavity threshold energy. Once the pump power increased over 310 mW, the mode-locked pulse trains started to split and finally reached the second order HML state, and maintained stably between 310 and 353 mW of the pump power. The Nonlinear growth of output power may be attributed to the fact that the oscillator and the pre-amplifier shared one pump. With the increase of the pump power, the seed source, injected into the pre-amplifier, was variable. The slope efficiency of the whole fiber laser system was around 12.28%.

3.1 HML operation

HML is a novel method to increase the repetition rate of laser. Conventionally, HML was conducted in anomalous dispersion regime [39, 40]. The oversaturation of the saturable absorber is the main mechanism resulting in multiple pulses or HML [24, 41]. Therefore, the long fiber length is conducive to achieve HML due to the higher pulse energy resulted from a low repetition rate. However, general fiber has a positive GVD near 1 μm, if without any dispersion compensation, pulse will propagate in ANDi regime and tolerate larger nonlinear phase shit, which is hard to achieve HML. To overcome this problem, the narrow bandwidth spectral filter is needed to assist formation of multiple pulses or HML [29, 42]. There are many reports about second order HML in ANDi regime [25, 26], and the higher order ANDi HML based on the narrow bandwidth cascade long period fiber grating (C-LPFG) [27, 28]. By using the FBG with a narrow bandwidth (0.71 nm), in the 2 m laser cavity, we achieved the second order HML based on SESAM. Figure 5a shows the typical HML pulse trains. The 6.835 ns of repetition period (146.3 MHz of repetition rate) was achieved. The standard deviation of pulse-to-pulse amplitude fluctuation was around 0.073%, indicating a good pulse stability. As shown as Fig. 5b, there is no obvious difference between HML AC trace and CWML AC trace, guarantying the pulse width in the HML state was still optimal for micro-machining of metals. Figure 5c is the RF spectrum of the second order harmonic pulses. The peak-to-pedestal was ~ 52 dB.

3.2 The repetition rate of pulse clusters

The repetition rate of pulse clusters depends on the division frequency signal of the AOM drive. By controlling the division frequency signal, the pulse clusters with tunable repetition rate were achieved. Figure 6 shows the pulse clusters with different repetition rate. In the CWML state, the repetition rate of pulse clusters was 7.315 MHz, 731.5 kHz and 73.15 kHz adjustable. Once the HML occurs, the repetition rate of pulse clusters become 1.463 MHz. The wider tuning range of repetition rate (7.315 MHz, 731.5 kHz, 73.15 kHz, 1.463 MHz) can provide a flexible machining speed that is positively correlated with the repetition rate.

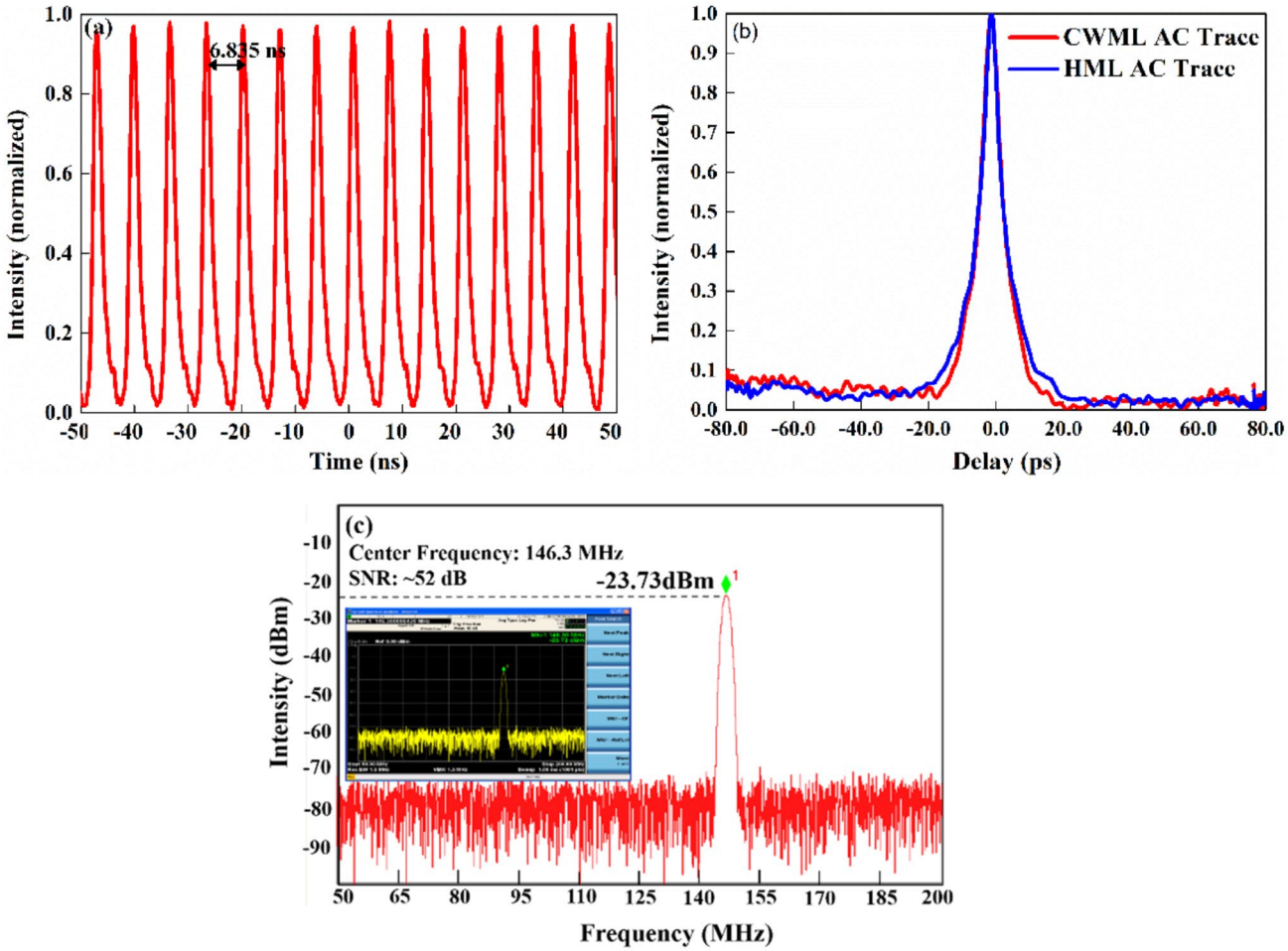

Fig. 5 **a** The typical harmonic mode-locked (HML) pulse trains, **b** autocorrelation trace, **c** frequency spectrum of the second order HML pulses

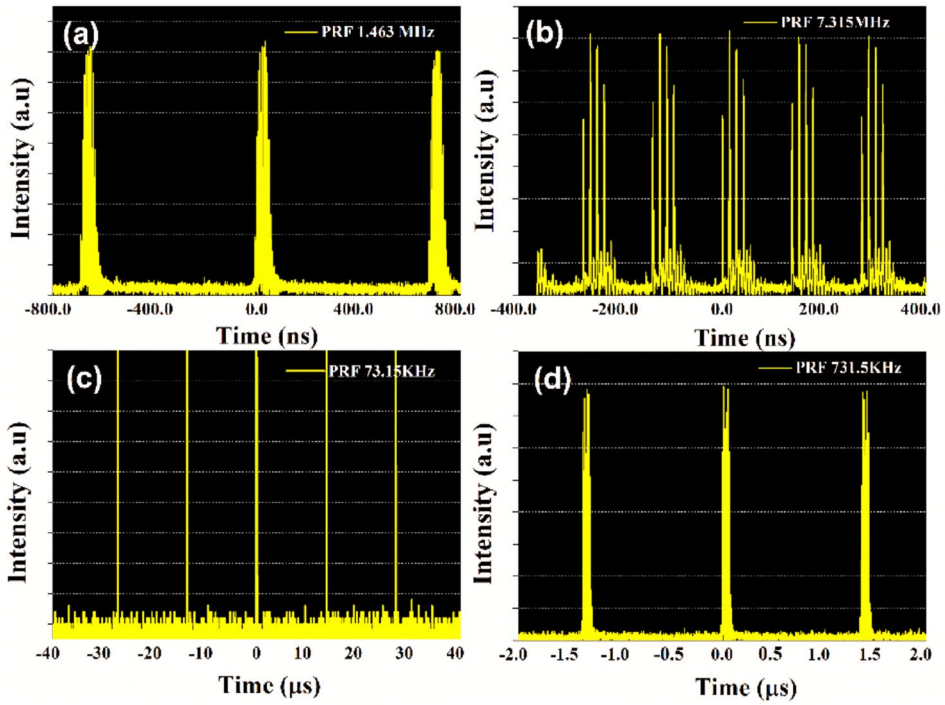

Fig. 6 Pulse clusters with different repetition rate **a** 1.463 MHz, **b** 7.315 MHz, **c** 731.5 kHz, **d** 73.15 kHz

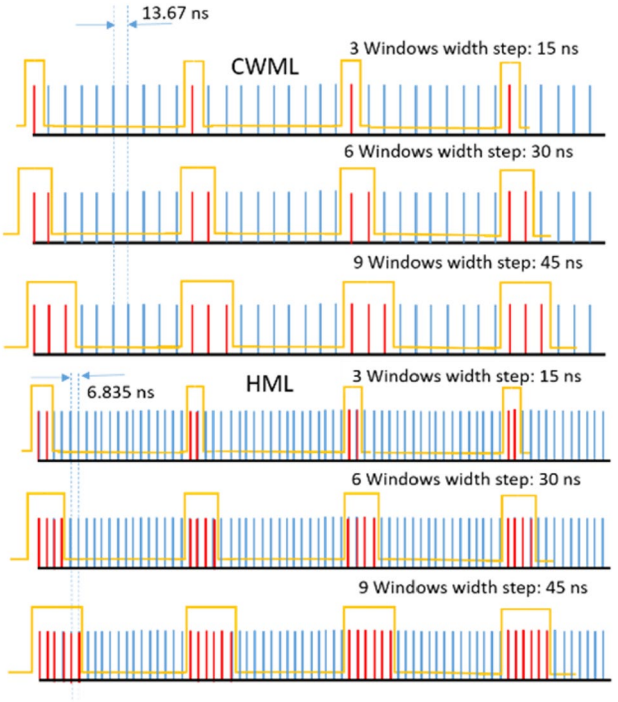

Fig. 7 The schematic diagram of setting step units

3.3 The number of pulses selection

The number of pulses in each pulse cluster can be controlled by the signal of window width and delay. A step unit of the windows width is 5 ns, which means that picking up single pulse from the pulse trains with a 13.67 ns of repetition period requires 3 step units. If 2, 3, 4, 5 and 6 pulses need to be picked, the step units should be 6, 9, 12, 15 and 18.In the HML state, the repetition period of pulses will become 6.835 ns. Therefore, 6, 9, 12, 15 and 18 step units can pick twice as many pulses as the CWML state. Figure 7 shows the schematic diagram of setting step units.

Figure 8 shows the different number of pulses picked from the pulse clusters with a 136.7 ns of repetition period. As shown as Fig. 9, in comparison to the previous result in the CWML state, the number of pulses was 6, 8, 10 and 12 tunable, indicating the tunability of the burst mode laser was improved.

Figure 9 also indicates that the pulse-to-pulse amplitude fluctuation in the HML state was smaller than that in the CWML state, the 4, 6, 8 pulses with nearly equal amplitude were obtained. This result was better than previous reports [10–16]. The same energy (same pulse amplitude) between

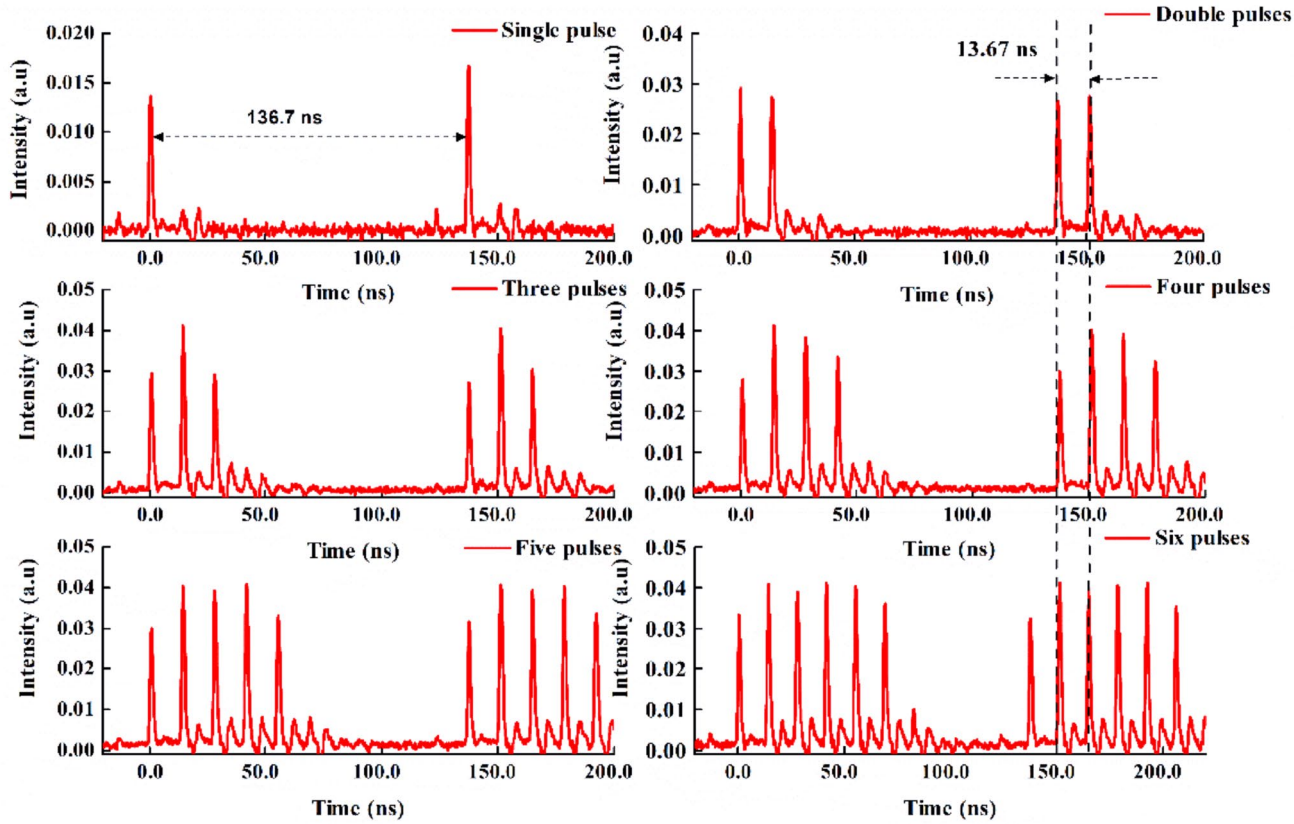

Fig. 8 Number of pulses of burst mode based on the CWML state

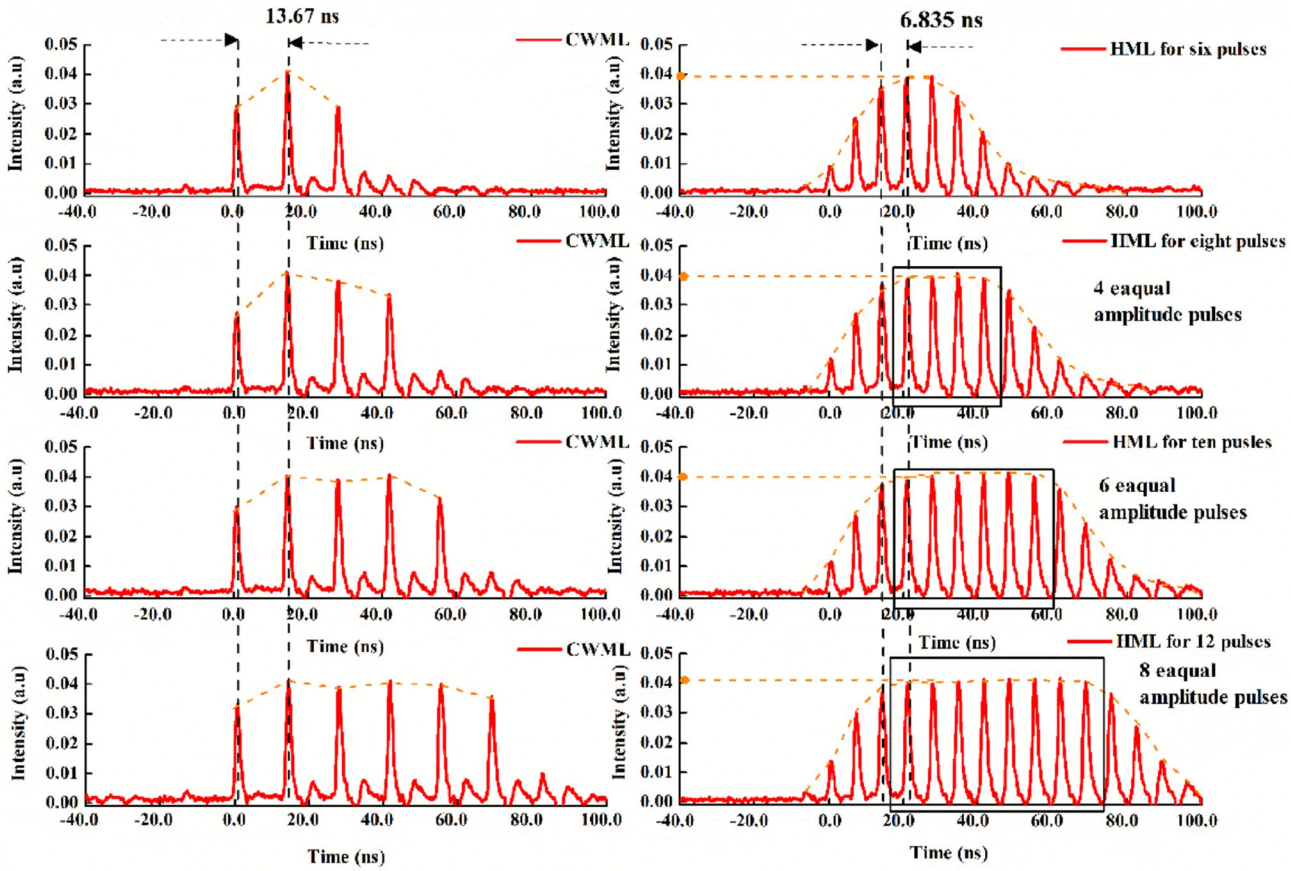

Fig. 9 Number of pulses of burst mode based on the HML state

pulses in per pulse cluster is very important for the stable micro-machining, since the energy of each pulse should be ensured to reach the ablation threshold of the metallic material. In addition, the amplitude of pulses at the edge of each pulse cluster are relatively low, which is caused by the mismatch between the rise time of the modulator and the repetition period of pulses. As shown in Fig. 10, the 20 ns rise time of modulator was longer than the 13.67 ns repetition period of pulses, the modulation window would cut off a part of pulse energy before it fully raised. And, the smaller the pulse repetition period was, the more pulse energy at the edge of pulse clusters would be excluded. Therefore, for a same pre-set modulation window of 30 ns, a worse result was observed when the system was the HML state (Fig. 10b, c).

4 Conclusions

In summary, we successfully demonstrated the setup of a 3.5 ps burst mode laser. By achieving the HML in ANDi regime, the tunability of the burst mode laser has been improved. The burst mode fiber laser is ideal for a flexible source due to its wide tuning range. When combined with amplification technology, the laser will exhibit good performance in metal micro-machining applications.

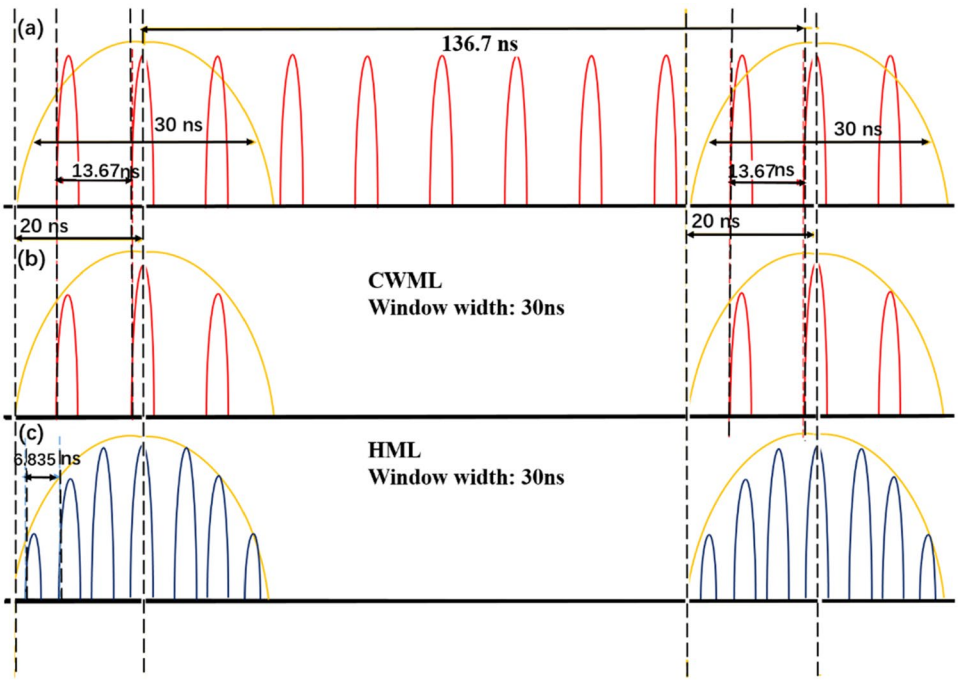

Fig. 10 Pulse selection principle diagram

Acknowledgements The authors would like to thank every member of School of Electronic Science and Engineering in Xiamen University and Nanguang Hi-Tech (Xiamen) Laser Co., Ltd.

Compliance with ethical standards

Conflict of interest The authors declare no conflicts of interest.

References

1. J. Kleinbauer, R. Knappe, R. Wallenstein, Appl. Phys. B Lasers Opt. **80**(3), 315–320 (2005)
2. H.Y. Lin, D. Sun, N. Copner, W.Z. Zhu, Opt. Mater. **69**, 250–253 (2017)
3. X. Liu, R.M. Osgood, Y.A. Vlasov et al., Nat. Photonics **4**(8), 557–560 (2010)
4. F. Dausinger, H. Hugel, V.I. Konov, Proc. SPIE **5147**, 106–115 (2003)
5. F. Dausinger, Proc. SPIE **5777**, 840–845 (2005)
6. M. Lapczyna, K.P. Chen, P.R. Herman et al., Appl. Phys. A Mater. Sci. Process. **69**(1), S883–S886 (1999)
7. A. Nebel, T. Hermann, B. Henrich, R. Knappe et al., Proc. SPIE **6108**, 610812 (2006)
8. H. Kalaycıoğlu, K. Eken, F.Ö. Ilday, Opt. Lett. **36**(17), 3383–3385 (2011)
9. H. Kalaycioglu, Ö. Akçaalan, S. Yavaş et al., J. Opt. Soc. Am. B **32**(5), 900–906 (2015)
10. G. Livescu, L.M.F. Chirovsky et al., Opt. Lett. **20**(22), 2324–2326 (1995)
11. C.W. Siders, J.L.W. Siders et al., App. Opt. **37**(22), 5302–5305 (1998)
12. L.L. Ming, M. Chen, G. Li, Appl. Phys. B **123**(5), 151 (2017)
13. R. Knappe, Proc. SPIE. **82430I**, 1–7 (2012)
14. Z.X. Bai, C. Yang, L.Y. Chen et al., Opt. Laser Technol. **46**, 25–28 (2013)
15. M.N. Slipchenko, J.D. Miller, S. Roy et al., Opt. Lett. **39**(16), 4735–4738 (2014)
16. P. Elahi et al., Opt. Lett. **39**(2), 236–239 (2014)
17. L.A. Gomes, L. Orsila, T. Jouhti et al., IEEE J. Sel. Top. Quantum Electron **10**(1), 129–136 (2004)
18. O. Katz, Y. Sintov, Opt. Commun. **281**(10), 2874–2878 (2008)
19. M. Zhang, L.L. Chen, C. Zhou et al., Laser Phys. Lett. **6**(9), 657–660 (2009)
20. F.Q. Lian, Z.W. Fan, X.F. Wang et al., Laser Phys. **21**(6), 1103–1107 (2011)
21. J. Liu, J. Xu, P. Wang, IEEE Photonics Technol. Lett **24**(7), 539–541 (2011)
22. J.B. Lecourt, S. Boivinet, Y. Hernandez, Proc. SPIE **8551**, 85510A (2012)
23. J.B. Lecourt, C. Duterte, F. Narbonneau et al., Opt. Express **20**(11), 11918–11923 (2012)
24. B. Ortac, A. Hideu, M. Brunel, Opt. Lett. **29**(17), 1995–1997 (2004)
25. J.L. Wang, X.B. Bu, R. Wang, Appl. Opt. **53**(23), 5088–5091 (2014)
26. L.J. Kong, X.S. Xiao, C.X. Yang, Chin. Phys. B **20**(2), 024207 (2011)
27. D.F. Liu, X.J. Zhu, C.H. Wang et al., IEEE Photonics Technol. Lett. **22**(23), 1726–1728 (2010)
28. X.J. Zhu, C.H. Wang, S.X. Liu et al., IEEE Photonics Technol. Lett. **24**(9), 754–756 (2012)
29. A. Haboucha, A. Komarov, H. Leblond, F. Sanchez, G. Martel, Opt. Fiber Technol. **14**(4), 262–267 (2008)
30. X.L. Li, C. Shang, Z.J. Yang et al., Asia Commun. Photonics Conf. (2018). https://doi.org/10.1109/ACP.2018.8595788
31. S.S. Huang, Y.G. Wang, P.G. Yan, Laser Phys. **24**(1), 015001 (2014)
32. F. Krausz et al., IEEE J. Quantum Electron **28**(10), 2097–2122 (1992)

33. H.A. Haus, IEEE J. Sel. Top. Quantum Electron **6**(6), 1173–1185 (2000)
34. X.L. Tian, M. Tang, X.P. Cheng et al., Opt. Express **17**(9), 7222–7227 (2009)
35. B. Ortaç, M. Plötner, J. Limpert et al., Opt. Express **15**(25), 16794–16799 (2007)
36. A. Agnesi, L. Carrà, F. Pirzio et al., J. Opt. Soc. Am. B **30**(11), 2960–2965 (2013)
37. C. Hönninger, R. Paschotta, F. Morier-Genoud et al., J. Opt. Soc. Am. B **16**, 46–56 (1999)
38. A. Agnesi, L. Carrà, C. Di Marco et al., IEEE Photonics Technol. Lett. **24**(11), 927–929 (2012)
39. F. Amrani, A. Haboucha, M. Salhi, Appl. Phys. B **99**(1–2), 107–114 (2010)
40. K. Guesmi, G. Semaan, M. Salhi et al., Rom. J. Phys. **61**(7–8), 1330–1338 (2016)
41. Y.J. Deng, W.H. Knox, Opt. Lett. **29**(18), 2121–2123 (2004)
42. G. Martel, C. Chédot, A. Hideur, P. Grelu, Fiber. Integr. Opt. **27**(5), 302–340 (2008)